Immobilization of the Plug Domain Inside the SecY Channel Allows Unrestricted Protein Translocation

Lycklama a Nijeholt, Jelger A.; Bulacu, Monica; Marrink, Siewert Jan ; Driessen, Arnold J.M.

Link to publication in University of Groningen/UMCG research database

Immobilization of the Plug Domain Inside the SecY Channel Allows Unrestricted Protein Translocation*

Jelger A. Lycklama a Nijeholt[‡], Monica Bulacu[§], Siewert Jan Marrink[§], and Arnold J. M. Driessen[‡1]

From the [‡]Molecular Microbiology, Groningen Biomolecular Sciences and Biotechnology Institute, and the Zernike Institute for Advanced Materials, University of Groningen, 9751 NN Haren, The Netherlands and [§]Molecular Dynamics, Groningen Biomolecular Sciences and Biotechnology Institute, and the Zernike Institute for Advanced Materials, University of Groningen, 9747 AG Groningen, The Netherlands

The SecYEG complex forms a protein-conducting channel in the inner membrane of *Escherichia coli* to support the translocation of secretory proteins in their unfolded state. The SecY channel is closed at the periplasmic face of the membrane by a small re-entrance loop that connects transmembrane segment 1 with 2b. This helical domain 2a is termed the plug domain. By the introduction of pairs of cysteines and crosslinkers, the plug domain was immobilized inside the channel and connected to transmembrane segment 10. Translocation was inhibited to various degrees depending on the position and crosslinker spacer length. With one of the crosslinked mutants translocation occurred unrestricted. Biochemical characterization of this mutant as well as molecular dynamics simulations suggest that only a limited movement of the plug domain suffices for translocation.

In the Gram-negative bacterium *Escherichia coli*, periplasmic and outer membrane proteins need to pass the inner membrane to arrive at their final location. This process is facilitated by the Sec translocase, a multisubunit complex with the SecYEG heterotrimer as a protein-conducting channel in the inner membrane (1). Through genetic, biochemical, and structural analysis, many of the intimate features of the translocation process have been resolved. Protein translocation requires a molecular motor SecA that associates with the SecYEG channel. SecA utilizes cycles of ATP binding and hydrolysis to guide unfolded secretory proteins (preproteins) into the SecYEG channel. Structural analysis has provided detailed insights in how this channel may be gated (2). Because the inner membrane of *E. coli* and other bacteria is an energy-transducing membrane, the translocation pore has to accommodate unfolded translocating polypeptides and at the same time maintain a tight seal to prevent unwanted leaks of protons and other ions across the membrane.

The structure of the *Methanococcus jannaschii* SecYEβ heterotrimer shows that the main subunit SecY consists of two halves with an internal pseudo-2-fold symmetry. The two SecY halves comprise transmembrane segments (TMS)[2] 1–5 and 6–10, respectively, and are connected by a hinge region. In this organization, the channel resembles a clamshell that encompasses a central hourglass-shaped pore with a narrow constriction ring in the middle of the membrane. This ring is lined by hydrophobic residues and is proposed to prevent leakage of ions in the closed state (3). SecE embraces the SecY clamshell at the hinge-side in a V-shaped manner. The third subunit, SecG or Secβ is peripherally associated with the SecYE complex.

In the *M. jannaschii* SecYEβ structure, the pore-like opening in the center is obstructed by a small helical re-entrance loop. This plug-like domain is also termed TMS 2a and resides at the periplasmic side of the constriction ring thereby closing the pore on the extracellular (or periplasmic) face of the membrane. In the clamshell organization of the SecY protein, the two halves contact each other via TMS 2, TMS 7, and TMS 8. The opening between TMS2 and TMS7/8 is termed the lateral gate and localizes at the front of the SecY pore. When opened it may provide an exit path for hydrophobic polypeptide segments to enter the membrane. The lateral gate also fulfils an important role in the channel opening mechanism during protein translocation (4). Insertion of the signal sequence into this lateral gate region may result in a widening of the central constriction and an opening of the channel. This in turn will destabilize the plug domain that once released from the extracellular funnel will vacate a central aqueous path for the translocation of preproteins.

Although the plug domain has been proposed to fulfil an important role in channel stability and opening, its exact function is not clear. *In vivo* crosslinking experiments using cysteine crosslinking suggests that the tip of TMS 2a contacts the C-terminal loop of SecE, which localizes more than 27 Å away from the central constrict region that it contacts in the *M. jannaschii* SecYEβ structure. To explain this discrepancy, it has been suggested that during channel opening, there is a considerable movement of the plug domain from near the center of the pore to the exterior on the periplasmic side of the membrane (5). *In vitro* crosslinking experiments show the same relocation of the plug to the periplasmic side, while SecYEG complexes in which the plug is immobilized outside the pore show an increased translocation activity (6). The latter is reminiscent of the activity of SecYEG complexes that contain signal sequence suppressor (*prl*) mutations, suggesting an involvement of the plug

---

[2] The abbreviations used are: TMS, transmembrane segment; IMV, inner membrane vesicle; DTT, dithiothreitol; BMOE, bis(maleimido)ethane; BMH, bis(maleimido)hexane; NaTT, sodium tetrathionate; MD, molecular dynamics.

domain in channel gating. Such *prl* mutations allow the translocation of signal sequence defective preproteins and are thought to be defective in proof reading of the preprotein. The proof reading mechanism includes the activation of SecA and the consecutive opening of the SecY pore. Interestingly, many of the *prlA* mutations in SecY localize to the central constriction region and the plug domain (7). Such *prlA* mutants show an increased affinity of SecA binding and a destabilized SecY-SecE interaction (8, 9). It is hypothesized that in *prlA* mutants the channel is destabilized allowing it to open more readily. In contrast, the wild-type SecY channel is highly stable and shows little ion conductance in the idle state (10). The *prl* -like phenotype of the SecY channel with the plug domain crosslinked to the C-terminal region of SecE, suggests that in the wild-type SecYEG the relocation of the plug is not a permanent movement. It also raises the question as to whether the plug domain in the crosslinking experiments moves to the external location accidentally or whether this movement is required to provide enough room for the translocating preprotein. In another study, the plug domain of the yeast Sec61α (which is homologous to SecY) has been deleted, and although this mutant is thermolabile, it is normally active in protein translocation (11). A structural study with the *M. jannaschii* SecYEβ suggests that upon the removal of the plug domain, another extracellular loop replaces the plug and orients toward the central constriction region (12). In the recent structure of a SecA-SecYEG complex stabilized by the transition state analogue of ATP hydrolysis, ADP-beryllium fluoride (BeFx), the central channel has opened partially. The plug domain was located more peripherally toward the periplasmic end of TMS 7, but still at a distance of 27 Å away from the SecE crosslinking site (13). This pre-open state may provide a site for the signal sequence to bind at an initial stage of translocation. It is, however, not known if this plug position is required for signal sequence binding nor has the actual movement of the plug domain during translocation been resolved.

To explore the dynamics of the presumed plug movement during translocation, we have used a cysteine-based crosslinking approach to immobilize the plug domain near the central constriction region to resemble its location in the closed state of the translocation channel. Through crosslinking with various spacer lengths we have evaluated the requirement for plug movement inside the SecY translocation pore. The data indicate that flexibility of the plug domain is a requirement for channel opening and only small movements are needed to allow protein translocation. Additionally, coarse-grained MD simulations support these biochemical findings.

EXPERIMENTAL PROCEDURES

Chemicals and Biochemicals—The isolation of inner membrane vesicles (IMVs) containing overexpressed levels of SecYEG and the purification of SecA, SecB, and proOmpA were performed as described (14). For translocation assays, proOmpA(290C) was labeled with fluorescein-maleimide (Invitrogen™) (15). Expression of OmpT and outer membranes isolation was as described (4). The hydrophilic oxidizer sodium tetrathionate (NaTT) was from Sigma and the bismaleimide crosslinking reagents bis(maleimido)ethane (BMOE)

and bis(maleimido)hexane (BMH) from Pierce. The reducing agent 1,4-dithiothreitol (DTT) was purchased from Roth. DNA restriction enzymes were obtained from Fermentas. All other chemicals were from Sigma.

Bacterial Strains and Plasmids—All strains and plasmids used are shown in Table 1. All cloning procedures were performed with DH5α cells. Site-directed mutagenesis employing the Stratagene QuikChange® kit was used to introduce cysteine mutations in the template vector pEK1 (16). For the construction of the double cysteine mutants, single cysteine constructs were used as templates. All introduced mutations were checked by sequencing. After cysteine introduction, the NcoI-ClaI secY fragment in the expression vector pEK20 was replaced for the mutated secY fragments. *E. coli* SF100 or NN100 were transformed with the indicated expression vectors and used for the overproduction of the different SecYEG mutant complexes.

Chemical Crosslinking and OmpT Assay—IMVs containing overexpressed levels of the cysteine-less or mutant SecYEG complexes were diluted to 1 mg/ml, and incubated for 30 min with NaTT, BMOE, or BMH (each at 1 mM final concentration) in a volume of 30 μl at 37 °C. Subsequently, the BMOE and BMH crosslinking was quenched with 10 mM DTT and incubated at 20 °C for 10 min. To determine the efficiency of intramolecular crosslinking, outer membrane vesicles containing overexpressed levels of OmpT were diluted to 1 mg/ml in 50 mM Tris-HCl, pH 8.0 and 0.3% (v/v) Triton X-100. The OmpT solution (5 μl) was mixed with the crosslinked and non-crosslinked IMVs (10 μl) and incubated for 30 min at 37 °C. Samples were loaded on 15% non-reducing SDS-PAGE and stained with Coomassie Brilliant Blue R250.

To access the plug position in the SecA-ADP-Beryllium fluoride (BeFx)-bound state, SecA (0.8 mg/ml) was incubated with 1.2 mg/ml IMVs in a buffer containing 20 mM HEPES/KOH pH 7.0, 50 mM KCL, 10 mM MgCl$_2$, 1 mM ADP, and with or without 2 mM BeSO$_4$ and 8 mM NaF. This solution was incubated for 30 min at 37 °C. To induce crosslinking, 2 mM NaTT, BMOE, or BMH were added to the solution. The suspension was incubated for various time intervals up to 10 min at 37 °C, and crosslinking was quenched by 1 mM (NaTT) or 5 mM (BMOE and BMH) DTT. SecY-SecA complex were dissociated by the addition of 50 mM EDTA and 1.5 M urea and incubated for 30 min at 37 °C. After dissociation, samples were treated with OmpT as described above.

MD Simulations—Because of the large size of the system and to the long time scale involved in the protein translocation through the Sec machinery, we have performed MD simulations by employing a coarse-grained representation of the SecYEG-SecA system. All the simulations were carried out with the GROMACS molecular dynamics package, using the version 2.1 of the MARTINI coarse-grained force field and its extension for proteins (17–19). This coarse-graining set-up has been previously used to simulate the behavior of other protein membranes (20, 21). The protein, the membrane, and the solvent were independently coupled to a heat bath of T = 310 K (time constant τ = 1 ps), while the system pressure was scaled semi-isotropically to p = 1 bar both in the plane of the membrane and perpendicular to the membrane (τ = 1 ps and compressibility β = 4.5 $\times$ 10^{-5} bar^{-1}). The crystal structure of SecYEG bound

to SecA from *T. maritima* (PDB entry 3DIN) was used as a starting configuration (13). This required re-creating the loop between TMS 2a (the plug) and TMS 1 (residues 42–61 from SecY) that are missing in the crystal structure. The other missing terminal residues (1–7 and 424–431 of SecY) were not reconstructed. To obtain the double cysteine mutant SecY, residues Phe-67 and Ser-394 (analogues of Phe-67 and Ser-405 from *E. coli*) were replaced with cysteine residues. The SecYEG protein was embedded in a pre-equilibrated POPC bilayer in water. At completion, a typical system consisted of 44356 coarse-grained particles: the protein complex (1353 amino acids for the SecYEGA), 1031 POPC lipids and, 27932 coarse-grained water particles (one coarse-grained water particle representing four real water molecules). Periodic boundary conditions in all directions were employed. For locating the protein in the membrane, the geometrical descriptions of Zimmer *et al.* (13) were followed. The membrane and the solvent were allowed to minimize the energy and to relax while imposing positional restrains on all the protein backbone beads with a force constant of 1000 kJ nm^{-2} mol^{-1} for 10 ns. After this, the system was further simulated without any restrains.

Besides the standard run parameters associated with the Martini force field, two extra harmonic potentials were considered between the side chains of the 67C and 394C mutated residues, to mimic the disulfide bond and the BMH crosslinkers. For the disulfide bond, an equilibrium length of 3.9 Å and an elastic constant $K = 5000$ kJ nm^{-2} mol^{-1} were used (19). For the BMH crosslinker a correspondent elastic bond had to be created. This was modeled by a more flexible bond with the equilibrium length of 15 Å and the elastic constant $K = 1500$ kJ nm^{-2} mol^{-1}, trying to mimic as closely as possible the lengths distribution of a BMH crosslinker reported in the atomistic simulations of Green *et al.* (22). The overall reduction in the number of degrees of freedom and the use of shorter range potentials makes the coarse grain model computationally very efficient: The systems described in this work were simulated with an integration time step of 20 fs, which corresponds to an effective time of 80 fs. This correction factor of four is used because, for the systems modeled using a coarse-grained representation, the dynamics is faster by comparison with the ones simulated in atomistic detail (the coarse-grained interactions are smoother than the atomistic interactions, and part of the effective friction from the atomic level is lost by coarse-graining. Following this convention, the simulations described in this work were run for 1.6 microseconds (effective time).

Other Techniques—*In vitro* translocation of proOmpA was performed as described (15) using 5 μg of IMVs. Translocation of fluorescein-labeled proOmpA was determined after protease digestion and SDS-PAGE by visualized with a Fujifilm LAS-4000 image analyzer. Excitation and emission filters were set at 460 and 510 nm, respectively. The SecA translocation ATPase activity was determined by measuring the amount of released free phosphate using the malachite green assay (23). Measurements were done in triplicate and corrected for background ATPase activity. Protein concentrations were determined with the Bio-Rad RC DC protein assay kit using bovine serum albumin as a standard.
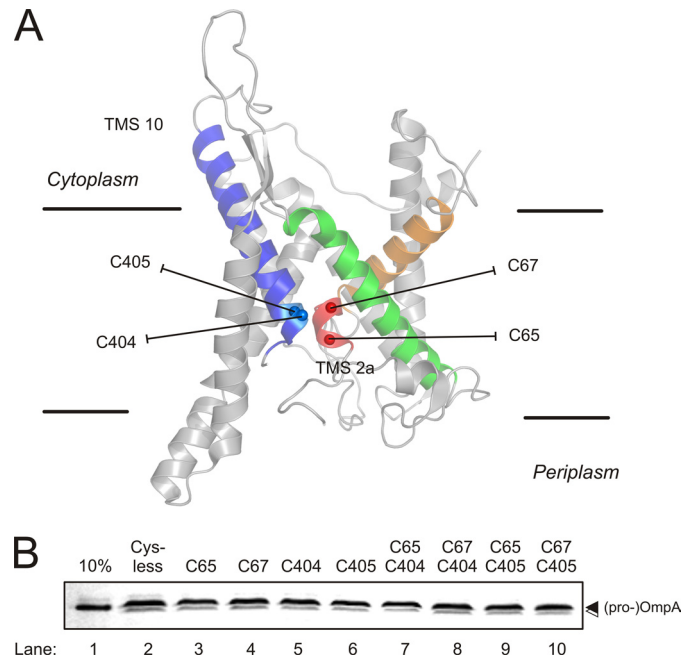

FIGURE 1. *A*, positions of the cysteine mutations introduced in TMS 2a (plug) (*red*) and TMS 10 (*blue*) introduced into the *E. coli* SecY and mapped on the structure of the *M. jannaschii* SecY. The two lateral gate helices TMS 2b and 7 are shown in *orange* and *green*, respectively. TMS 8 and 9 are removed for clarity. *B*, translocation of fluorescein-proOmpA by inner membrane vesicles containing overexpressed levels of SecYEG with the indicated single and double cysteine mutants of SecY.

RESULTS

Introduction of Cysteines in the Plug Domain and TMS10 of SecYEG—Previous cysteine crosslinking analysis suggests that the plug domain is completely displaced from the periplasmic exit funnel of SecYEG and moves toward the SecE clamp to contact the C-terminal tail of SecE. To explore the extent of plug movement we introduced unique cysteine pairs in SecY to immobilize the plug domain inside the channel in its resting closed position. Using the structure of SecYEβ from *M. jannaschii* and an alignment to the *E. coli* SecYEG, two residues located on the plug domain (Asn-65, Phe-67) and two residues in TMS 10 (Thr-404, Ser-405) were chosen as these are predicted to be in close proximity in the closed SecY channel (Fig. 1*A*). The plug domain connects TMS 1 with TMS 2a, and is part of the N-terminal clam-domain of SecY, whereas TMS 10 is part of the C-terminal clam domain. Moreover, the cysteine positions in TMS 10 localize close to the middle region of the channel. Thus, the immobilization of the plug by cysteine-directed crosslinking is expected to prevent the release of the plug from its central pore position. The targeted amino acid residues were pair wise replaced by cysteines using a site-directed mutagenesis approach with the cysteine-less SecYEG vector as template. This resulted in four different pairs of plug and TMS 10 mutants (Table 1). The SecYEG mutants were cloned into an expression vector, and plasmids were introduced in *E. coli* strain SF100. After growth, IMVs were isolated and analyzed by SDS-PAGE. The different SecYEG mutant complexes were expressed to similar levels as the cysteine-less SecYEG complex (data not shown). Likewise, the *in vitro* proOmpA translocation activity of these IMVs as assayed in the presence of dithiothre-

TABLE 1
Strains and plasmids used in this study

Strains/plasmids	Characteristics	Source (Ref.)
E. coli DH5α	*supE44, ΔlacU169 (Δ80lacZ_M15) hsdR17, recA1, endA1, gyrA96 thi-1, relA1*	(25)
E. coli SF100	*F⁻, ΔlacX74, galE, galK, thi, rpsL, strA, ΔphoA(pvuII), ΔompT*	(26)
E. coli NN100	SF100, *unc⁻*	(27)
pET36	proOmpA(245C)	F. Bonardi, unpublished results
pEK1	Cysteine-less SecY	(16)
pEK20	Cysteine-less SecYEG	(16)
pEK20-65C	SecY(N65C)EG	This study
pEK20-67C	SecY(F67C)EG	This study
pEK20-404C	SecY(T404C)EG	This study
pEK20-405C	SecY(S405C)EG	This study
pEK20-65C-404C	SecY(N65C, T404C)EG	This study
pEK20-65C-405C	SecY(N65C, S405C)EG	This study
pEK20-67C-404C	SecY(F67C, T404C)EG	This study
pEK20-67C-405C	SecY(F67C, S405C)EG	This study

itol (reducing conditions) was similar (Fig. 1*B*). This demonstrates that the cysteine mutants did not adversely affect the activity of the translocase.

Crosslinking of the Plug Domain TMS2a to TMS10—To immobilize the plug domain, IMVs harboring overexpressed levels of various SecYEG mutants were oxidized with the hydrophilic agent NaTT. To visualize the intramolecular disulfide bond formation, we used the previously developed OmpT assay (4). OmpT protease cleaves between arginine 255 and 256 in the cytoplasmic loop that connects TMS 6 and TMS 7. This results in the formation of an N- and C-terminal SecY fragment with calculated molecular masses of 28 and 20 kDa, respectively. On SDS-PAGE, the fragments migrate at apparent molecular masses of 25 and 18 kDa, respectively (Fig. 2). Upon oxidation (or crosslinking) of the cysteines in TMS 2a (plug) and TMS 10, OmpT treatment should result in a cleaved product that on SDS-PAGE migrates as the full-length SecY but that upon reduction dissociates in the two expected fragments. The cysteine-less SecYEG was completely cleaved both under oxidizing (+NaTT) and reducing (+DTT) conditions with the appearance of the expected N- and C-terminal SecY fragments and a loss of full-length SecY (Fig. 2). When the single cysteine mutants were used, similar results were obtained (data not shown). Incubation of the double cysteine mutants of SecYEG with the oxidizer NaTT resulted in high crosslinking efficiencies up to 90% (Fig. 2, *lane 3*). When the OmpT-treated NaTT-oxidized IMVs were incubated with DTT, SecY dissociated into the two expected fragments (Fig. 2, *lane 4*). These data demonstrate that the selected positions in the plug domain are in close proximity to TMS 10 and validate the predictions based on the structure of the SecYEβ channel. It should be noted that even in the absence of the oxidizing agent NaTT, a portion of double cysteine SecY mutants migrated as full-length protein upon OmpT treatment (Fig. 2, *lane 2*). This suggests that these cysteines readily form a disulfide bond consistent with their close proximity in the SecY structure.

Next, the IMVs were incubated with various sized covalent crosslinkers to immobilize the plug domain at different distances from the back of the channel. Herein, the chemical crosslinkers BMOE and BMH were used that introduce a spacer between the thiol groups of up to 8 and 13 Å, respectively. To maximize the chemical crosslinking, IMVs were first reduced with DTT, re-isolated, and subsequently treated with BMOE and BMH. With BMOE, crosslinking efficiencies were

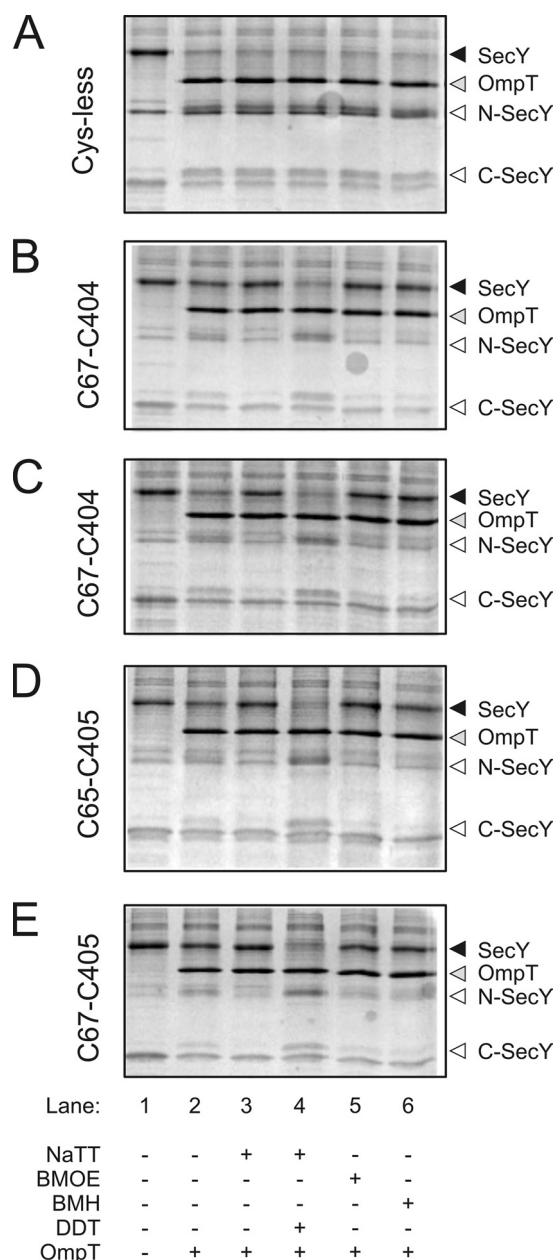| Lane:	1	2	3	4	5	6
NaTT	-	-	+	+	-	-
BMOE	-	-	-	-	+	-
BMH	-	-	-	-	-	+
DDT	-	-	-	+	-	-
OmpT	-	+	+	+	+	+

FIGURE 2. **IMVs containing the different SecYEG mutants were treated with NaTT, BMOE, and BMH (1 mM) and the crosslinking efficiency was checked by OmpT treatment.** The intensity of the full-length SecY bands were compared for the OmpT-treated and untreated conditions. As a control, all the disulfide bonds are reduced by the addition of 10 mM DTT (*lane 4*).
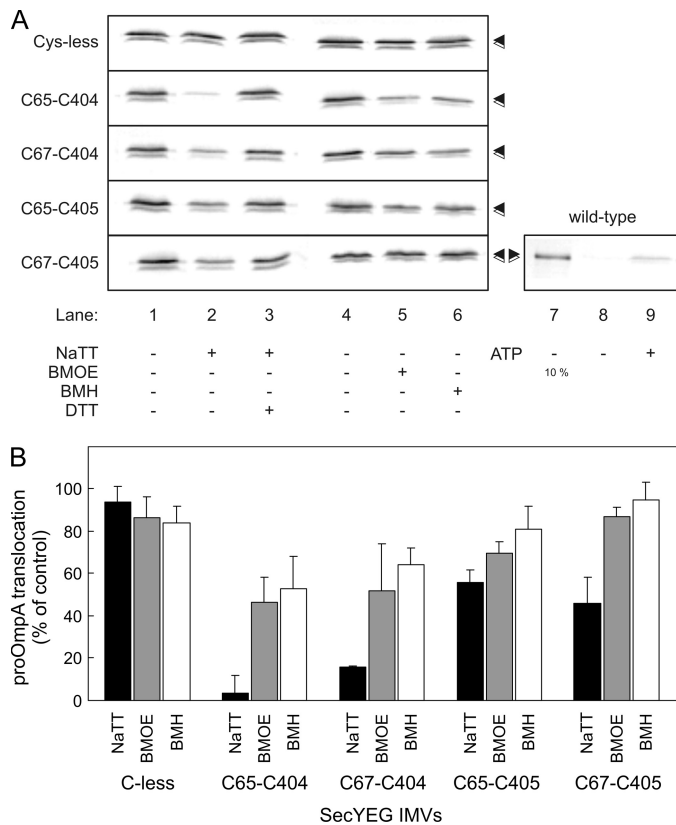
FIGURE 3. *A*, ProOmpA translocation by the indicated IMVs reduced with DTT (*lanes 1* and *4*), oxidized with NaTT (*lane 2*), oxidized with NaTT and reduced with DTT (*lane 3*), crosslinked with BMOE (*lane 5*), or crosslinked with BMH (*lane 6*). In *lane 8*, ATP was omitted from the reaction, whereas in *lane 9*, wild-type vesicles without overexpression of the SecYEG complex were used. *B*, quantitation of the translocation reactions by IMVs oxidized with NaTT (*black bars*), crosslinked with BMOE (*gray bars*) or BMH (*white bars*). Reactions were related to the translocation by untreated IMVs.

FIGURE 4. *A*, SecA ATPase activity of the indicated cysteine-less, single and double cysteine mutants of SecYEG. *B*, effect of NaTT (*black bars*), crosslinking with BMOE (*dark gray bars*) or BMH (*white bars*) on the SecA translocation ATPase activity of IMVs (*light gray bars*) harboring the different SecYEG mutants.

comparable to that observed with the oxidizer NaTT of up to 90%. BMH showed slightly lower crosslinking efficiency to about 70–80% (Fig. 2, *lanes 5* and *6*). These data suggest that the plug TMS2a/TMS 10 region is relatively dynamic allowing the efficient introduction of long chemical crosslinkers.

Protein Translocation Activity of SecYEG Mutants with an Immobilized Plug Domain—The effect of plug immobilization on translocation was determined by *in vitro* translocation assays using fluorescein-labeled proOmpA as a substrate. NaTT-induced oxidation of SecY(C65,C404)EG and SecY(C67,C404)EG nearly completely abolished the translocation activity down to the background levels (Fig. 3*A*, *lane 2*). These background levels of translocation are due to the presence of the endogenous wild-type SecYEG complex as shown by the control (Fig. 3*A*, *lane 9*). In contrast, proOmpA translocation by the cysteine-less SecYEG complex was unaffected by the NaTT-induced oxidation. Remarkably, the SecY(C65,C405)EG and SecY(C67,C405)EG mutants were only partially inhibited by the oxidation. With all mutant pairs, the proOmpA translocation activity was restored after DTT-induced reduction of the disulfide bonds (Fig. 3*A*, *lane 3*). These data show that the disulfide-bonded immobilization of the plug domain in the closed state of the SecYEG complex inactivates the translocation channel.
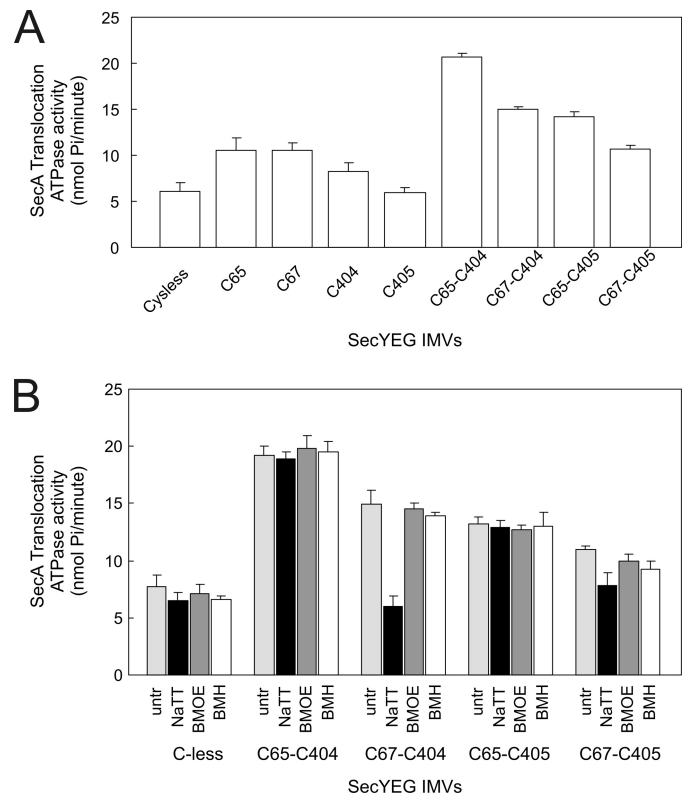
To investigate the degree of freedom in the plug domain movement, the translocation activity was tested with SecYEG complexes harboring the covalent thiol-specific crosslinkers BMOE and BMH. With each mutant pair, the proOmpA translocation activity was higher for the BMOE-crosslinked complexes compared with the NaTT-oxidized SecYEG complexes (Fig. 3*A*, compare *lanes 5* and *2*), whereas BMOE had no effect on the translocation activity of the cysteine-less SecYEG. With the more flexible BMH crosslinker a similar or further restoration of the proOmpA translocation activity was observed. Remarkably, the SecY(C67,C405)EG mutant showed normal levels of translocation activity when crosslinked with BMOE and BMH. These data suggest that the SecYEG channel tolerates the immobilization of the plug domain provided that a certain degree of motional flexibility is retained.

Plug Domain Movement and SecA ATPase Activation Are Not Mechanistically Coupled—In a previous study, we have shown that the lateral gate opening of SecYEG and the preprotein-dependent activation of the SecA ATPase activity are allosterically linked (4). To investigate whether such a mechanistic link also exists with plug domain movement, the proOmpA stimulated SecA ATPase activity was assayed in the presence of IMVs containing the various crosslinked SecYEG mutants. Under reducing conditions, most of the double cysteine mutants of SecYEG showed an elevated level of proOmpA-stimulated SecA ATPase activity compared with the cysteine-less SecYEG complex. This effect appears largely due to the cysteine mutation in the plug domain as shown by an analysis of the single cysteine mutants in the plug domain and TMS 10 (Fig. 4*A*).
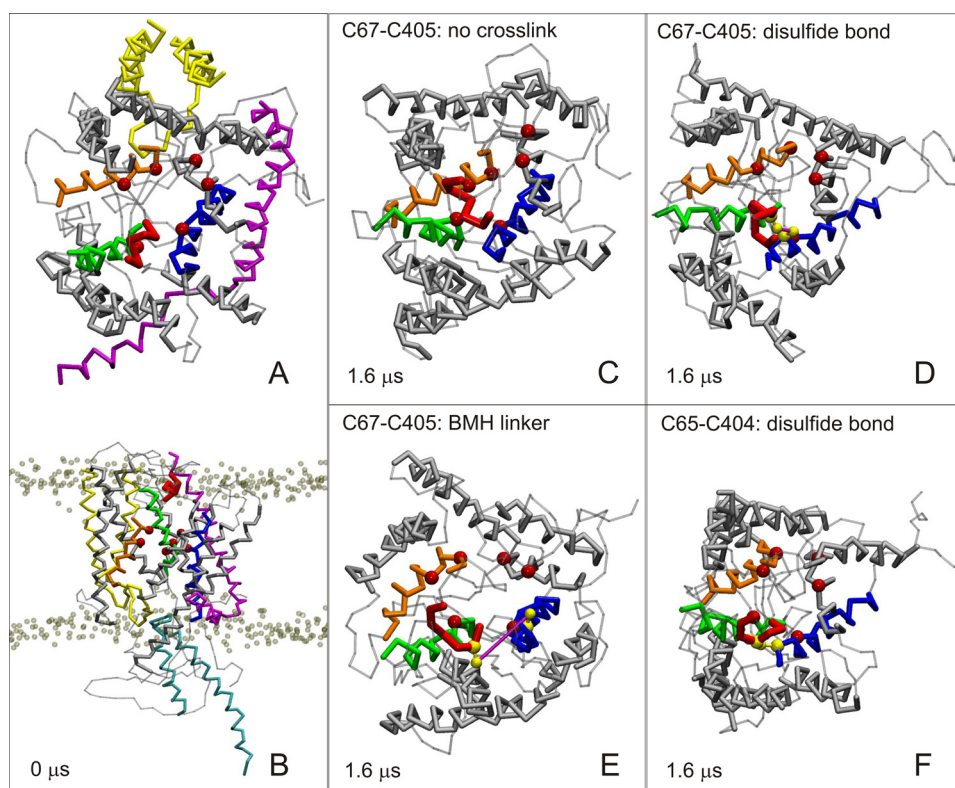
FIGURE 5. **MD simulation of the plug domain positions in cross-linked and native SecY.** MD starting configuration of the SecYEGA complex embedded in a fully hydrated POPC membrane: top (*A*) and lateral (*B*) views. SecY is pictured in *gray* except for highlighted parts: the plug is *red*, the helices forming the lateral gate are *orange* (TM2b) and *green* (TM7), and the helix TM10 is *blue*. The residues forming the hydrophobic ring are depicted as *red beads*. SecE, SecG, and SecA (only its two-helix finger) subunits are represented in *yellow*, *magenta*, and *cyan*, respectively. For clarity, the water molecules are omitted, and the membrane is represented only by the phosphate groups (transparent beads in the lateral view). *Top views* of the SecY protein at the end of 1.6 microsecond MD simulations in different setups: no crosslinks (*C*), disulfide crosslink between Cys-67 and Cys-405 (*D*), BMH crosslink between Cys-67 and Cys-405 (*E*), and disulfide crosslink between Cys-65 and Cys-404 (*F*). *Yellow beads* represent the mutated cysteine residues connected by an elastic bond (in *magenta*).

bound to the SecYEG complex. For clarity, however, a small part of SecA (the two-helix finger entering SecYEG) is shown in Fig. 5*B*. Even though molecular dynamics simulations cannot aim to model entirely the protein translocase mechanism, we focus mainly on the plug position in the funnel and the overall conformation of the SecYEG channel. If the plug does not hinder the channel and the conformation resembles an open conformation, we consider translocation favorable.

The two cysteine mutations F67C and T394C were introduced in the *T. maritima* SecY corresponding to the residues 67 and 405 of the *E. coli* SecY. First, the entire complex was simulated without any bonds between the two cysteines. When we compare the starting conformation, which represents the crystal structure, and the simulation after 1.6 μs, the overall structure appears stable in time (compare Fig. 5, *A* and *C*). While the plug domain acts as a flexible small helix, it stays at a certain position near the periplasmic end of the proposed lateral gate during the simulation. The lateral gate and the pore ring itself adopt a more closed state, although a moderate flexibility allows breathing of both parts. Additional simulations were performed with a disulfide bond or a BMH linker between the two cysteines. We found that when we introduced the BMH linker between residues 67 and 394, the overall conformation remained more open, when compared with the simulation without crosslink introduced (compare Fig. 5, *C* and *E*). In contrast, a disulfide bond between Cys-67 and Cys-394 adopts a more closed conformation (Fig. 5*D*). Furthermore, when we introduced cysteines at positions 65 and 393 (corresponding with Cys-65 and Cys-404 in *E. coli*), introduction of a disulfide bond resulted in a similar closed conformation as with the previous mutant (compare Fig. 5, *D* and *F*). Thus, these data show that in contrast to the disulfide bonding of the plug domain with TMS 10, BMH crosslinking results in a more open conformation of the SecYEG channel, providing an explanation for the observed translocation activity.

Flexibility of the Plug Domain in the SecA-bound SecYEG Complex—In the crystal structure of the *T. maritima* SecA-SecYEG a displacement of the plug domain of SecY is observed toward the periplasmic end of TMS 7 (13). In this state, the distance between the thiol groups of the introduced cysteines in the plug and TMS 10 ranges from 14–16 Å, which is significantly longer that what can be bridged by BMOE. In addition, Cys-65 and Cys-67 in the helical segment of the plug domain

Immobilization of the plug domain in the channel through oxidation or chemical crosslinking of the double cysteine mutants of SecY(C65, C404) and SecY(C65, C405) did not affect the SecA translocation ATPase (Fig. 4*B*). In the case when a disulfide bond is introduced using Cys-67, a slight decrease in SecA ATPase activity was observed. These data demonstrate that the preprotein-stimulated SecA ATPase activity and plug domain movements are mechanically unlinked.

Molecular Dynamics Simulation of the Crosslinking Induced Containment of the Plug Domain Movement—To better understand the effect of crosslinking of the plug domain at the molecular level, molecular dynamics simulations were performed. Herein, the channel plasticity and plug domain flexibility were analyzed for the different crosslinked states and compared with the native state. As a starting configuration, we used the x-ray structure of the "SecA-bound" form of the *T. maritima* SecYEG that corresponds to a pre-open state (13). In this configuration, the plug helix is deviated from the center of the channel toward the periplasmic side of the membrane; the lateral gate is partly open; and the six hydrophobic amino acids of the central constriction still form a semi-obstructive ring in the pore (see Fig. 5, *A* and *B*). The simulated system consists of the SecYEG channel with bound SecA embedded in a fully solvated POPC membrane. Throughout the simulation, the SecA motor remained
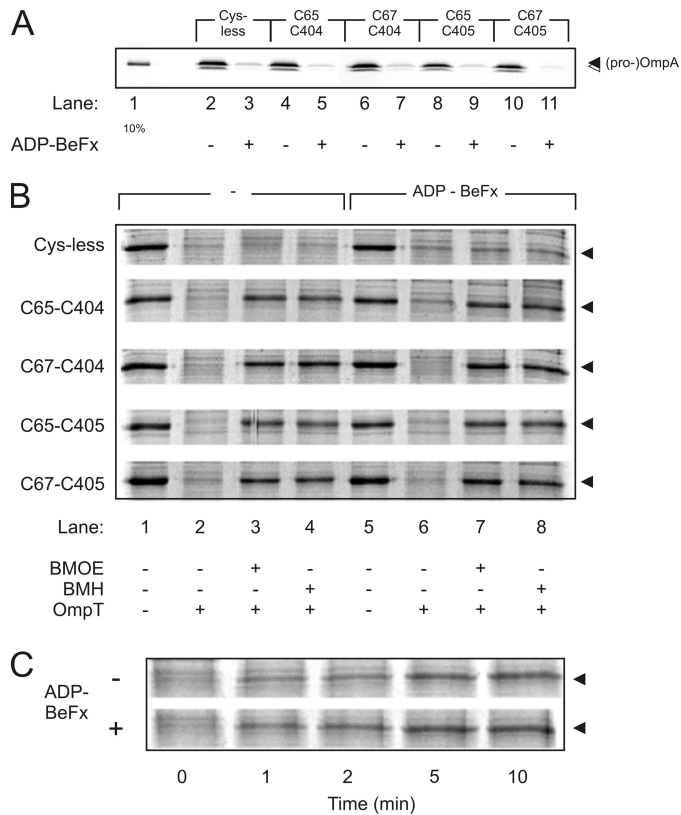
A

B

C

FIGURE 6. *A*, ProOmpA translocation activity of IMVs containing the SecY-SecA complex trapped in a transition state by ADP and beryllium fluoride. *B*, BMOE and BMH crosslinking of SecYEG-SecA and SecYEG-SecA-ADP-BeFx complexes assayed by OmpT cleavage. IMVs were incubated for 5 min with the indicated crosslinker, and reactions were subsequently quenched with 10 mM DTT. After removal of SecA by urea treatment, crosslinking was assessed by the OmpT protease assay. Only the Coomassie Brilliant Blue-stained SecY bands are shown. *C*, kinetics of BMH-induced crosslinking of SecY(67C,405C)EG-SecA complexes incubated with and without ADP-BeFx. Crosslinking was quenched at the indicated times with DTT whereupon the samples were treated with OmpT.

have opposed orientations. To follow plug displacement, the crosslinkers were used as molecular rulers. Herein, the SecA-SecYEG complex was trapped in a transition state by the addition of ADP and beryllium fluoride. This resulted in a near to complete (> 95%) inhibition of proOmpA translocation (Fig. 6*A*), demonstrating that the translocation sites are blocked. Next, the covalent crosslinker BMOE or BMH was added to the SecA-SecYEG complex stabilized by ADP and beryllium fluoride and native SecA-SecYEG complexes. After 5 min, the reactions were quenched with DTT, and upon the addition of OmpT, the extent of crosslinking was estimated from the amount of full-length SecY detected by SDS-PAGE. Crosslinking efficiencies were similar for the trapped and native SecA-SecYEG complex (Fig. 6*B*). Also when the kinetics of crosslinking was followed in time by quenching the crosslinker at various time intervals after addition, no significant difference was observed (Fig. 6*C*). In addition, we also tested the crosslinking efficiency of the SecY(C67,C405)EG mutant bearing a stalled proOmpA-Dhfr intermediate (4). Irrespective of the crosslinker used (NaTT, BMOE, or BMH), the formation of a translocation intermediate did not significantly affect the crosslinking efficiency (data not shown). Taken together, these data suggest that the plug domain is highly flexible.

DISCUSSION

Here we investigated the dynamics of the plug domain of the SecYEG protein-conducting channel. Structural analysis of SecYEG suggests that the tip of the plug (TMS 2a) domain and TMS 10 are in close proximity when the pore is in the closed state. By introducing cysteines into TMS 2a and 10, the plug could efficiently be immobilized through the formation of a disulfide bond confirming that these amino acid residues are indeed in close proximity. It is important to note that in this crosslinked state an intramolecular crosslink is formed between the two SecY halves. Thus, the crosslink is expected to interfere with a channel-opening mechanism that involves separation of the two SecY halves to open a central aqueous pore. Indeed with specific cysteine pairs, the disulfide-bonded immobilization of the plug resulted in a near to complete inhibition of the translocation activity. This is in line with a previous study that showed when the plug domain is crosslinked to TMS 7 via a disulfide bond, the translocation activity is reduced to background levels (24). Surprisingly, our study also shows that with the SecY(C65,C405)EG and SecY(C67,C405)EG mutants translocation activity was only partially inhibited despite a near to complete oxidation. Therefore, disulfide bonding of the plug domain close to the interior of the channel only inactivates translocation in a position-specific manner. To allow for a greater flexibility, crosslinking experiments were also performed with the chemical crosslinkers BMOE and BMH that contain a spacer with a length of 8 and 13 Å, respectively. Remarkably, this resulted in a restoration of the translocation activity relative to the disulfide-bonded state and the activity increased with the spacer length of the crosslinking agent. With the SecY(C67,C405)EG mutant, the BMOE and BMH crosslinking of the plug to TMS 10 resulted in an uninhibited proOmpA translocation activity. Taken together, this demonstrates that a certain degree of flexibility is required to allow movement of the plug domain during protein translocation.

In our studies, the movement of the crosslinked plug is restricted by the crosslinker length to distances that prevent the presumed long range movement (6) in which the tip of the plug needs to move entirely to a putative binding site at the C-terminal region of SecE. The latter hypothesis reasoned that this plug movement is needed to allow preproteins to pass an entirely unrestricted pore. However, it is likely that the observed crosslinks to the C-tail of SecE do not represent a long-term location of the plug domain, but are rather caused by the flexibility of the plug domain. The plug may infrequently shift to this periplasmic localization whereupon it is trapped at the SecE C-terminal region by the crosslinker. This crosslinked SecY protein shows Prl-like phenotype, which is characterized by an elevated activity of SecY. This was not observed in our studies when the plug domain was crosslinked to the middle region of the translocation channel, further suggesting that the C-terminal tail of SecE is not a long-term location of the plug domain.

A previous study showed that intramolecular disulfide crosslinking of the lateral gate of SecYEG resulted in an inactivation of the SecA translocation ATPase activity, whereas introduction of flexibility into the lateral gate region through

the use of longer spacer length crosslinkers resulted in a restoration of the translocation ATPase (4). This indicates that lateral gate opening and activation of the SecA ATPase are allosterically linked processes. We addressed the same question with the crosslinking-induced immobilization of the plug domain in the central channel. However, we noted that already the introduction of cysteine mutations in TMS 2a and 10 resulted in an elevated SecA ATPase activity. This phenomenon was also observed with some of the single cysteine mutants (Cys-65, Cys-67, and Cys-404) but more pronounced when the two cysteine mutations were present in these domains. With most mutants, oxidation or chemical crosslinking had little effect on the SecA translocation ATPase. We therefore conclude that plug domain movement and SecA ATPase activation are not directly linked.

To obtain more insight in the freedom of motion of the plug domain in the channel of SecY channel, we carried out molecular dynamics simulations with the SecYEG-SecA of *T. maritima* embedded in a POPC membrane as a starting configuration (13). We introduced the cysteine pair corresponding to the *E. coli* SecY(C67,C405)EG. The coarse-grained simulations were run for 1.6 μs and we observe that within this time frame the plug domain remained in the vicinity of the periplasmic end of TMS 7 (Fig. 5*C*). Also we observe that the channel adopts a more compact state, thereby closing the lateral gate and the pore ring to a certain extent. When we introduce a disulfide bond between the cysteines on the plug domain and TMS 10, the simulation shows a similar compact state of the channel, but the plug domain still has the degrees of freedom to reach the periplasmic end of the lateral gate (Fig. 5*D*). On the contrary, when we introduce a BMH linker, the channel adopts a more open state, thereby providing an explanation for the unrestricted translocation opposed to the disulfide-immobilized plug domain (Fig. 5*E*). It could be that the BMH because of its dimensions prevents closing of the preopen state. Furthermore, when we introduce cysteines at positions homologous to 65C and 404C in *E. coli*, we see a similar closed state as with the previous mutant when a disulfide is introduced (compare Fig. 5, *D* and *F*). The difference in ability to translocate proOmpA for these two mutants when the plug domain is immobilized by a disulfide bond is difficult to extract from these simulations. The observation that the first mutant is only partially (50%) impaired in translocation, while the latter is totally inhibited, could be an effect of a different orientation of the plug domain or the connecting TMS 10. We conclude that the MD simulations correlate well with the functional data, providing insights in the effect of the immobilized plug domain on the overall conformation of the channel. Overall these data suggest that the movement of the plug domain required to allow for protein translocation is not more than 13 Å, which is substantially less than the 27 Å needed to reach the C terminus of SecE. In addition, the location where the plug domain ends up after SecA binding in the crystal structure is still 27 Å away from the C terminus of SecE, namely at the periplasmic side of the lateral gate. It is therefore difficult to envision that the plug domain would move away from this location to the SecE tip in subsequent steps in the translocation, which is all the way on the other side of the channel.

REFERENCES

1. Driessen, A. J., and Nouwen, N. (2008) *Annu. Rev. Biochem.* **77,** 643–667
2. Van den Berg, B., Clemons, W. M., Jr., Collinson, I., Modis, Y., Hartmann, E., Harrison, S. C., and Rapoport, T. A. (2004) *Nature* **427,** 36–44
3. Gumbart, J., and Schulten, K. (2008) *J. Gen. Physiol* **132,** 709–719
4. du Plessis, D. J., Berrelkamp, G., Nouwen, N., and Driessen, A. J. M. (2009) *J. Biol. Chem.* **284,** 15805–15814
5. Harris, C. R., and Silhavy, T. J. (1999) *J. Bacteriol.* **181,** 3438–3444
6. Tam, P. C., Maillard, A. P., Chan, K. K., and Duong, F. (2005) *EMBO J.* **24,** 3380–3388
7. Smith, M. A., Clemons, W. M., Jr., DeMars, C. J., and Flower, A. M. (2005) *J. Bacteriol.* **187,** 6454–6465
8. Duong, F., and Wickner, W. (1999) *EMBO J.* **18,** 3263–3270
9. van der Wolk, J. P., Fekkes, P., Boorsma, A., Huie, J. L., Silhavy, T. J., and Driessen, A. J. M. (1998) *EMBO J.* **17,** 3631–3639
10. Saparov, S. M., Erlandson, K., Cannon, K., Schaletzky, J., Schulman, S., Rapoport, T. A., and Pohl, P. (2007) *Mol. Cell* **26,** 501–509
11. Junne, T., Schwede, T., Goder, V., and Spiess, M. (2006) *Mol. Biol. Cell* **17,** 4063–4068
12. Li, W., Schulman, S., Boyd, D., Erlandson, K., Beckwith, J., and Rapoport, T. A. (2007) *Mol. Cell* **26,** 511–521
13. Zimmer, J., Nam, Y., and Rapoport, T. A. (2008) *Nature* **455,** 936–943
14. van der Does, C., de Keyzer, J., van der Laan, M., and Driessen, A. J. M. (2003) *Methods Enzymol.* **372,** 86–98
15. de Keyzer, J., van der Does, C., and Driessen, A. J. (2002) *J. Biol. Chem.* **277,** 46059–46065
16. van der Sluis, E. O., Nouwen, N., and Driessen, A. J. (2002) *FEBS Lett.* **527,** 159–165
17. Hess, B., Kutzner, C., van der Spoel, D., and Lindahl, E. (2008) *J. Chem. Theory Computat.* **4,** 435–447
18. Marrink, S. J., Risselada, H. J., Yefimov, S., Tieleman, D. P., and de Vries, A. H. (2007) *J. Phys. Chem. B* **111,** 7812–7824
19. Monticelli, L., Kandasamy, S. K., Periole, X., Larson, R. G., Tieleman, D. P., and Marrink, S. J. (2008) *J. Chem. Theory Computat.* **4,** 819–834
20. Sengupta, D., Rampioni, A., and Marrink, S. J. (2009) *Mol. Membr. Biol.* **26,** 422–434
21. Yefimov, S., van der Giessen, E., Onck, P. R., and Marrink, S. J. (2008) *Biophys. J.* **94,** 2994–3002
22. Green, N. S., Reisler, E., and Houk, K. N. (2001) *Protein Sci.* **10,** 1293–1304
23. Lill, R., Dowhan, W., and Wickner, W. (1990) *Cell* **60,** 271–280
24. Maillard, A. P., Lalani, S., Silva, F., Belin, D., and Duong, F. (2007) *J. Biol. Chem.* **282,** 1281–1287
25. Hanahan, D. (1983) *J. Mol. Biol.* **166,** 557–580
26. Baneyx, F., and Georgiou, G. (1990) *J. Bacteriol.* **172,** 491–494
27. Nouwen, N., van der Laan, M., and Driessen, A. J. M. (2001) *FEBS Lett.* **508,** 103–106